16th World Conference on Earthquake, 16WCEE 2017

Santiago Chile, January 9th to 13th 2017

Paper N° 3401 (Abstract ID)

Registration Code: S-D1464689697

NON-STATIONARY STOCHASTIC DYNAMICS RESPONSE ANALYSIS OF BILINEAR OSCILLATORS TO PULSE-LIKE GROUND MOTIONS

A. Giaralis[(1)], I. Kougioumtzoglou[(2)], K. Dos Santos[(3)]

[(1)] *Senior Lecturer, Dept. of Civil Engineering, City University London, London, UK, agathoklis@city.ac.uk*
[(2)] *Assistant Professor, Dept. of Civil Engineering and Engineering Mechanics, Columbia University, NY, USA, iak2115@columbia.edu*
[(3)] *PhD Candidate, Dept. of Civil Engineering and Engineering Mechanics, Columbia University, NY, USA, kmd2191@columbia.edu*

Abstract

A non-stationary stochastic averaging/linearization formulation is considered in conjunction with a phenomenological stochastic model for pulse-like ground motions (PLGMs) to probe into the response of bilinear hysteretic strain hardening oscillators to typical near-source accelerograms with forward-directivity signatures without resorting to non-linear response history analysis (NRHA). In particular, the considered stochastic PLGM model is parametrically defined by a non-separable non-stationary stochastic process treating the high and the low frequency content of typical PLGMs in a consistent manner as a superposition of “bursts” of energy on the time-frequency plane with different amplitude, duration, bandwidth, location in time, and location in frequency. Each such burst is represented by a uniformly modulated non-stationary process of the separable kind. Further, the adopted stochastic dynamics formulation yields time-varying equivalent linear properties (ELPs) which are construed as non-stationary stochastic processes with evolutionary statistics dependent on the time-evolving intensity and frequency content of the PLGM stochastic excitation. It is numerically demonstrated by considering a PLGM stochastic process fitted to a typical fault-normal recorded accelerogram with a single forward-directivity low-frequency pulse that the ELPs derived by the proposed approach for various different bilinear oscillators are amenable to a clear physical interpretation: they can be viewed as instantaneous (time-varying) effective stiffness and viscous damping characterizing the time-varying inelastic response level/behavior whose severity is governed by resonance structural dynamics phenomena related to the input seismic energy distribution on the time-frequency plane and to the pre-yield natural period of the bilinear oscillators. Furthermore, it is verified in the context of Monte Carlo analysis pertaining to an ensemble of 250 simulated PLGM records compatible with the adopted PLGM stochastic model that the peak inelastic response of bilinear oscillators can be well approximated by the peak response of equivalent linear oscillators defined by appropriate statistics of ELPs evaluated at the time instant when the response variance determined by the adopted approach is maximized. Overall, the herein reported numerical data illustrates the usefulness and applicability of the proposed approach to serve as a potent alternative tool in assessing the seismic vulnerability of yielding structures to PLGMs within the performance-based earthquake engineering framework compared to the currently used approaches relying on NRHA. At first instance, the herein presented approach can be adopted within a stochastic incremental dynamic analysis context to account for the influence of forward-directivity effects to seismic structural response.

Keywords: stochastic pulse-like seismic ground motion model; non-stationary stastical linearization; non-staionary equivalent linear properties; simulation of pulse-like ground motions; bilinear hysteretic oscillator

1. Introduction

Seismological considerations suggest that, under certain conditions, horizontal earthquake ground motions (GMs) recorded close to the seismic fault and along the fault normal direction may exhibit one or more long period high-amplitude pulse(s) mostly attributed to the so-called forward-directivity effects (e.g., [1,2]). Such pulses have been identified and extracted from databanks of near-source recorded GMs using various signal processing tools (e.g., [3-5]). Importantly, these low frequency pulses may carry a significant fraction of the total GM energy imposing considerable ductility demands to relatively flexible structures having natural periods close to the dominant pulse period (e.g., [6-8]). In this regard, significant recent research efforts have been devoted to assess the vulnerability of structures to pulse-like ground motions (PLGMs) within a probabilistic performance-based earthquake engineering context (e.g., [9-11]). This is typically accomplished by conducting nonlinear response history analyses (NRHA) in which the seismic input action is represented either by ensembles of recorded PLGMs out of the limited number of PLGMs available in GM databanks. Alternatively, artificial simulated accelerograms with pulse-like signatures may also be used (e.g., [12]). In the latter case, the high frequency content is modelled via standard stochastic models commonly employed to model far-field GMs, while the pulses (low frequency content) are modelled by superposing empirical analytically defined deterministic functions (waveforms) in the time domain (e.g., [2,13]).

Herein, an alternative, considerably different, stochastic dynamics approach is proposed to study the inelastic response of bilinear hysteretic single-degree-of-freedom (SDOF) oscillators exposed to typical PLGMs without conducting NRHA. This is achieved by using a non-stationary stochastic dynamics-based formulation [14,15] in conjunction with a recently proposed phenomenological stochastic model which represents the salient features of PLGMs [16]. Specifically, the adopted stochastic dynamics formulation couples concepts of the classical stochastic averaging technique applied to bilinear hysteretic oscillators with strain hardening [17] with a non-stationary statistical linearization approach [18] to derive time-varying equivalent linear properties (ELPs). These ELPs can be viewed as non-stationary stochastic processes with evolutionary statistics dependent on the input stochastic excitation and, from a theoretical viewpoint, they serve as effective stiffness (or equivalently natural frequency) and viscous damping ratio in the definition of an underlying equivalent linear damped SDOF system (ELS). Further, the considered stochastic PLGM model is parametrically defined by a non-separable non-stationary stochastic process treating the high and the low frequency content of typical PLGMs in a consistent manner as a superposition of "bursts" of energy on the time-frequency plane with different amplitude, duration, bandwidth, location in time, and location in frequency (see also [19,20]).

The main aim of this work is to numerically verify that the derived ELPs pertaining to bilinear oscillators with different properties and exposed to the PLGM model bear a physical significance and can be treated as instantaneous (time-varying) stiffness and viscous damping ratio whose values reflect the severity of non-linear response at different times during the earthquake excitation. For a typical PLGM input, it is expected that tracing in time the inelastic response of relatively flexible bilinear oscillators through these ELPs can serve as a potent structural dynamics approach for peak inelastic response prediction. To assess the validity of this argument, a Monte Carlo-based analysis is further undertaken herein, in which peak ductility demands are approximated by peak linear responses of appropriately defined ELSs through ELP statistics for a large ensemble of simulated PLGMs generated as realizations of the underlying PLGM model along the lines in [21,22]. The remainder of this paper is structured as follows. Section 2 reviews the adopted stochastic dynamics formulation and discusses important mathematical and numerical aspects. Section 3 presents the herein considered PLGM stochastic model and describes an efficient simulation strategy for artificial PLGMs. Section 4 applies the proposed approach to various bilinear oscillators for a PLGM model fitted to a particular recorded GM with significant forward directivity effects and provides comprehensive numerical evidence on the usefulness and applicability of the approach. Finally, Section 5 summarizes conclusions and points to future research directions.

2. Stochastic averaging treatment of bilinear hysteretic oscillators

Consider a viscously damped quiescent bilinear hysteretic single-degree-of-freedom (SDOF) oscillator with mass *m*, viscous damping constant *c*, yielding deformation u_y, pre-yield stiffness *k*, and post-yield over pre-yield stiffness ratio a. Its response to a zero-mean non-stationary seismic ground acceleration stochastic process $a_g(t)$ is governed by the stochastic differential equation given as

$$\ddot{u}(t)+2\xi_o\omega_o\dot{u}(t)+\frac{f_h\left(u(t),\dot{u}(t)\right)}{m}=-a_g(t). \tag{1}$$

In the above equation, $u(t)$ denotes the displacement response of the oscillator relative to the ground motion, $\omega_o=(k/m)^{1/2}$ is the pre-yield natural frequency, $\xi_o= c/2\omega_o m$ is the critical damping ratio and a dot over a symbol represents differentiation with respect to time t. Further, the function f_h represents the oscillator restoring force following a bilinear hysteretic law which can be mathematically written as

$$f_h\left(u(t),\dot{u}(t)\right)=aku(t)+(1-a)kz(t). \tag{2}$$

In the above equation $z(t)$ is an auxiliary state variable governed by the following differential equation [23]

$$\dot{z}(t)=u_y\dot{u}(t)\left[1-H\left(\dot{u}(t)\right)H\left(z(t)-1\right)-H\left(-\dot{u}(t)\right)H\left(-z(t)-1\right)\right], \tag{3}$$

in which $H(v)$ is the Heaviside step function, assuming the values $H(v)=1$ for $v\geq 0$ and $H(v)=1$ for $v<0$.

Focusing on lightly damped bilinear oscillators (e.g. $\xi<0.10$), it can be assumed that the response process $u(t)$ in Eq. (1) exhibits a pseudo-harmonic behavior described by the system of equations [17]

$$u(t)=A(t)\cos\left[\omega(A)t+\varphi(t)\right] \quad ; \quad \dot{u}(t)=-\omega(A)A(t)\sin\left[\omega(A)t+\varphi(t)\right], \tag{4}$$

where the response amplitude process, $A(t)$, and the phase, $\varphi(t)$, are slowly varying functions in time and, thus, they can be treated as constant over one cycle of oscillation. Next, manipulation of the system of Eqs. (4) yields

$$A^2(t)=u^2(t)+\frac{\dot{u}^2(t)}{\omega^2(A)}. \tag{5}$$

To this end, the classical statistical linearization framework [18] is herein adopted to define a surrogate equivalent linear system (ELS) such that the variance of its response displacement process $y(t)$ to the stochastic process $a_g(t)$ approximates well the response variance $u(t)$ of the hysteretic oscillator considered in Eq. (1). Specifically, the governing equation of motion of the ELS reads as

$$\ddot{y}(t)+\omega_{eq}^2(A)y(t)+\beta_{eq}(A)\dot{y}(t)=-a_g(t), \tag{6}$$

which corresponds to a linear damped SDOF oscillator with effective natural frequency and viscous damping properties (ELPs) $\omega_{eq}(A)$ and $\beta_{eq}(A)$, respectively. The above ELPs are functions of the time-dependent inelastic response amplitude $A(t)$ in Eq. (5) and are expressed as

$$\omega_{eq}^2(A)=a\omega_o^2+\frac{k_{eq}(A)}{m} \quad ; \quad \beta_{eq}(A)=2\xi_o\omega_o+\frac{c_{eq}(A)}{m}. \tag{7}$$

The terms $k_{eq}(A)$ and $c_{eq}(A)$ appearing in Eq. (7) correspond to the contributions of the hysteretic part of the response expressed by the function f_h in Eq. (2) to the effective stiffness and viscous damping properties of the ELS in Eq. (6). They are given by the expressions [17,18]

$$k_{eq}(A)=\frac{(1-a)k}{A}C_h(A) \quad ; \quad c_{eq}(A)=\frac{(1-a)k}{A\omega(A)}S_h(A) \tag{8}$$

where $C_h(A)$ and $S_h(A)$ are obtained in closed-form as

$$C_h(A)=\begin{cases}\frac{A}{\pi}\left(\Lambda-0.5\sin(2\Lambda)\right), & A>u_y\\ A, & A\leq u_y\end{cases} \quad ; \quad S_h(A)=\begin{cases}\frac{4u_y}{\pi}\left(1-\frac{u_y}{A}\right), & A>u_y\\ 0, & A\leq u_y\end{cases}, \tag{9}$$

in which cos(Λ)=1-2u_y/A. In deriving Eqs. (7) to (9), an error function (difference) between Eqs. (4) and (6), that is, between the governing equations of the hysteretic oscillator and of the ELS, has been defined and minimized in the mean square sense (see [17,18] for detailed derivations).

Next, attention is focused on the ELPs $\omega_{eq}(A)$ and $\beta_{eq}(A)$ in Eq. (7) which are treated as non-stationary stochastic processes. This consideration is justified by noting that the ELPs are functions of the amplitude $A(t)$ of the inelastic response process $u(t)$, which is a non-stationary stochastic process itself. In this regard, the time-varying statistics of the ELPs, such as the mean value and standard deviation, can be obtained by applying the mathematical expectation operator $E_A[\cdot]$ with respect to the process $A(t)$. For instance, the time-varying mean values of the ELPs in Eq. (7) are given by the expressions

$$\omega_{eq}(t)=E_A\left[\omega_{eq}(A)\right] \quad ; \quad \beta_{eq}(t)=E_A\left[\beta_{eq}(A)\right] \tag{10}$$

The evaluation of the above expectations requires considering an underlying time-varying probability density function (PDF), $f(A,t)$, characterizing the evolutionary statistical attributes of the amplitude process $A(t)$. Following [14], it is assumed that $A(t)$ has the time-dependent Rayleigh distribution

$$f(A,t)=\frac{A(t)}{\sigma_u^2(t)}\exp\left(-\frac{A(t)^2}{2\sigma_u^2(t)}\right), \tag{11}$$

where $\sigma_u^2(t)$ is the non-stationary variance of the hysteretic response process $u(t)$. The choice of the above PDF $f(A,t)$ is motivated by the fact that the non-stationary PDF of the response amplitude of a linear lightly damped SDOF oscillator subject to Gaussian white noise excitation follows a time-dependent Rayleigh distribution of the form of Eq. (11), observing the property

$$\lim_{t\to\infty} f(A,t)=\frac{A}{\varsigma^2}\exp\left(-\frac{A^2}{2\varsigma^2}\right), \tag{12}$$

where ς^2 is the stationary response variance of the SDOF oscillator [24]. Furthermore, it is shown in [14] that the PDF in Eq. (11) is applicable to non-linear oscillators under evolutionary stochastic excitations, as well. By adopting the PDF in Eq. (11), the time-varying ELPs in Eq. (7) become functions of the non-stationary variance of the bilinear oscillator $\sigma_u^2(t)$, and, therefore, the governing equation of motion of the ELS in Eq. (6) becomes

$$\ddot{y}(t)+\beta_{eq}\left(\sigma_u^2(t)\right)\dot{y}(t)+\omega_{eq}^2\left(\sigma_u^2(t)\right)y(t)=-a_g(t). \tag{13}$$

Furthermore, a combination of deterministic and stochastic averaging yields the following first order stochastic differential equation for the bilinear hysteretic response amplitude (e.g. [14])

$$\dot{A}(t)=K_1(A,t)+K_2(A,t)w(t), \tag{14}$$

where

$$K_1(A,t)=-\frac{1}{2}\beta_{eq}\left(\sigma_u^2(t)\right)A(t)+\frac{\pi S\left(\omega_{eq}\left(\sigma_u^2(t)\right),t\right)}{2A\omega_{eq}^2\left(\sigma_u^2(t)\right)} \quad ; \quad K_2(A,t)=-\sqrt{\frac{\pi S\left(\omega_{eq}\left(\sigma_u^2(t)\right),t\right)}{\omega_{eq}^2\left(\sigma_u^2(t)\right)}}, \tag{15}$$

and $w(t)$ is a zero-mean white noise stochastic process of intensity one. In Eq. (15), $S(\omega,t)$ is the evolutionary power spectral density function (EPSD) characterizing the acceleration strong ground motion process $a_g(t)$ in the domain of frequencies ω. In the next section, an EPSD modelling acceleration ground motions with forward-directivity (pulse-like) effects is discussed and used in Eq. (15) in the ensuing numerical work. The solution of the stochastic differential equation in Eq. (14) proceeds by considering the associated Fokker-Planck equation governing the evolution of the response amplitude PDF $f(A,t)$ written as (e.g. [25])

$$\frac{\partial}{\partial t}f\left(A,t+\Delta t\middle|A',t\right)=-\frac{\partial}{\partial A}\left[K_1(A,t)f\left(A,t+\Delta t\middle|A',t\right)\right]+\frac{1}{2}\frac{\partial^2}{\partial A^2}\left[K_2^2(A,t)f\left(A,t+\Delta t\middle|A',t\right)\right] \tag{16}$$

Substituting the Rayleigh PDF of Eq. (11) into Eq. (16) and manipulating yields the following equation for the evolution of the non-linear system response variance (see [14] for a detailed derivation)

$$\dot{\sigma}_u^2(t) = -\beta_{eq}\left(\sigma_u^2(t)\right)\sigma_u^2(t) + \frac{\pi S\left(\omega_{eq}\left(\sigma_u^2(t)\right),t\right)}{\omega_{eq}^2\left(\sigma_u^2(t)\right)}. \tag{17}$$

The latter is a first-order ordinary differential equation, which can be solved by any standard numerical integration scheme such as the Runge-Kutta method. Once the evolution of the non-linear response variance $\sigma_u^2(t)$ is numerically determined, the non-linear response amplitude PDF of Eq. (11) can be readily obtained as well as the statistics of the time-varying ELPs in Eq. (7), such as their mean values in Eq. (10). In Section 4, time-dependent ELPs determined by taking as input the stochastic model for pulse-like strong ground motions discussed in the next section are used to probe into the seismic response of yielding bilinear hysteretic SDOF systems accounting for forward directivity effects without resorting to nonlinear response history analyses.

3. Stochastic representation and simulation of pulse-like ground motions

For the purposes of this work, the stochastic dynamics approach presented in the previous section is coupled with the phenomenological parametric stochastic model introduced by Lungu and Giaralis [16] capturing the salient time-varying features of pulse-like ground motions (PLGMs) in intensity and frequency content. This stochastic model relies on the common phenomenological interpretation of typical near-fault ground motion acceleration records with forward directivity effects as a superposition of relatively high frequency (HF) energy content on distinctive low frequency (LF) high energy pulses [2,13]. In the time domain, the model reads as [16]

$$a_g(t) = \sum_{i=1}^{P\geq 1} e_{HF_i}(t) g_{HF_i}(t) + \sum_{j=1}^{R\geq 1} e_{LF_j}(t) g_{LF_j}(t). \tag{18}$$

and is a superposition of P+R uncorrelated separable uniformly modulated non-stationary stochastic processes yielding an overall non-separable stochastic model (see also [19,20]). The first P processes (i.e., first term in Eq. (18)) model the evolution of the HF content of the PLGM stochastic model. Each of these processes are defined as a product of a stationary zero-mean stochastic process $g_{HFi}(t)$ (i =1,2,.., P), represented by a power spectrum density function $G_{HFi}(\omega)$ in the frequency domain, and a deterministic time-dependent envelope function $e_{HFi}(t)$. Similarly, the second term in Eq. (18) models the evolution of the LF content as a superposition of R stationary zero-mean stochastic processes $g_{LFj}(t)$ (j =1,2,.., R), represented by a power spectrum density function $G_{LFj}(\omega)$ in the frequency domain, each one uniformly time modulated via the time-varying envelope function $e_{LFj}(t)$.

In this study, the widely used Clough-Penzien (CP) two-sided spectrum defined for positive frequencies as

$$G_{HFi}(\omega) = \frac{\omega_{gi}^4 + 4\zeta_{gi}^2\omega^2\omega_{gi}^2}{\left(\omega_{gi}^2 - \omega^2\right)^2 + 4\zeta_{gi}^2\omega_{gi}^2\omega^2} \frac{\omega^4}{\left(\omega_{fi}^2 - \omega^2\right)^2 + 4\zeta_{fi}^2\omega_{fi}^2\omega^2}, \omega \leq \omega_{\max} \tag{19}$$

is used to model the frequency content of each of the i-th HF processes in Eq. (18) where ω_{max} is the highest frequency of interest. The CP spectrum comprises two linear filters in tandem: a high pass filter, characterized by the cut-off frequency ω_{fi} and the steepness (slope of the filter) ζ_{fi} and the Kanai-Tajimi filter, which accounts for the local soil conditions by representing soil deposits via a linear SDOF oscillator with (soil) natural frequency ω_{gi} and (soil) damping ratio ζ_{gi}. The role of the high pass filter is to eliminate spurious low frequencies allowed by the Kanai-Tajimi filter. Furthermore, the skewed bell-shaped function

$$e_{HF_i}(t) = C_{HF_i} t \exp\left(-\frac{b_i t}{2}\right) \tag{20}$$

is considered to model the time varying intensity of the HF stochastic processes in Eq. (18) commonly used for the task at hand (e.g. [26]). In the above equation, the parameter C_{HFi} relates to the peak amplitude of the envelope, while b_i controls the time instant at which the envelop attains its peak value (at $2/b_i$), as well as the width of the envelop. The latter has a non-linear relationship with the effective duration of each HF process defined as the time-interval in which 90% of the total process energy is released as discussed in [27].

The frequency content of the *j*-th LF process in Eq. (18) is modelled by the symmetric half-cosine two-sided spectrum defined for positive frequencies as [16]

$$G_{LF_j}(\omega)=\frac{1}{2}\left(1+\cos\left(\frac{\pi}{\mathrm{a}_j\omega_{pj}}\left(\omega-\omega_{pj}\right)\right)\right),\ \omega_{pj}\left(1-\mathrm{a}_j\right)\le\omega\le\omega_{pj}\left(1+\mathrm{a}_j\right), \tag{21}$$

where the parameter a_j controls the width and the peak value of the spectrum, and ω_{pj} is the dominant (central) frequency of the *j*-th pulse. Moreover, the time variation of each LF process is defined by the envelope function

$$e_{LF_j}(t)=C_{LF_j}\exp\left(-\frac{1}{2}\left(\frac{\omega_{pj}}{\gamma_j}\left(t-t_{pj}\right)\right)^2\right), \tag{22}$$

which is extensively used for modelling forward directivity pulses in the time domain (e.g. [13]). In the previous equation, C_{LFj} controls the amplitude of the LF content, t_{pj} is the time instant of the peak amplitude of the *j*-th function, while the parameter $\gamma_j>1$ takes on sufficiently large values such that the frequency content of the envelope function does not interfere with the frequency content of the LF part of the process in Eq. (18), that is, the support of the Fourier magnitude spectrum of the function in Eq. (22) falls outside the bandwidth of all the G_{LFj} spectra defined in Eq. (21).

Under the assumption that all the envelope functions involved in the definition of the *R*+*P* uncorrelated processes in Eq. (18) vary slowly and smoothly in time, the PLGM process $a_g(t)$ can be represented on the time-frequency plane by the EPSD (e.g., [20])

$$S(t,\omega)=\sum_{i=1}^{P}\left|e_{HF_i}(t)\right|^2 G_{HFi}(\omega)+\sum_{j=1}^{R}\left|e_{LF_j}(t)\right|^2 G_{LF_j}(\omega). \tag{23}$$

The above expression motivates the interpretation of the herein adopted stochastic PLGM model as a superposition of HF and LF energy bursts on the time-frequency plane, the LF bursts corresponding to distinct directivity pulses. Furthermore, Eq. (23) suggests that it is possible to generate artificial pulse-like ground motions compatible with a given non-separable EPSD $S(t,\omega)$ in an efficient manner by employing any standard stationary spectrum compatible simulation technique [28]. This is accomplished by, first, generate stationary time-histories compatible with all the different *R*+*P* spectra $G_{HFi}(\omega)$ and $G_{LFi}(\omega)$, then, multiply each time-history with the corresponding envelopes $G_{HFi}(\omega)$ and $G_{LFi}(\omega)$ to obtain time-histories with time-domain non-stationarity, and, finally, add (superpose) the previous non-stationary time-histories to derive pulse-like records with non-stationarity in both the time and frequency domain. Figure 1 depicts pictorially the above EPSD compatible simulation for the simplest case of *R*=*P*=1 (see [16]).

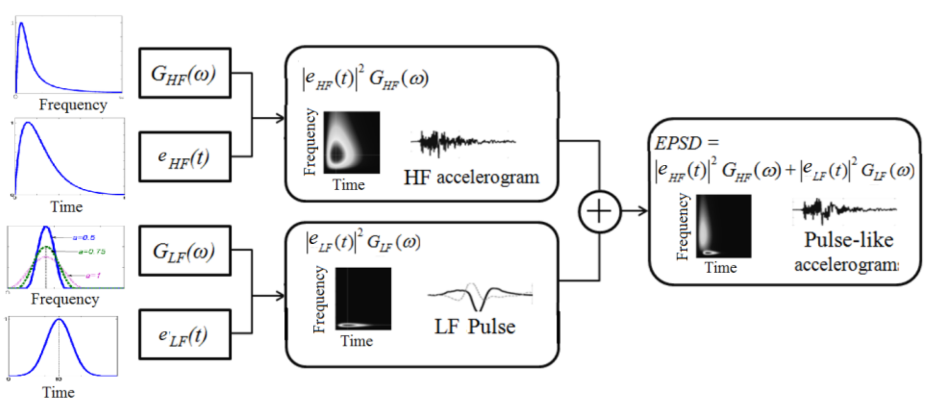

Fig. 1 – Generation of pulse-like accelerograms as realizations of the stochastic model in Eq. (18) for *R*=*P*=1.

4. Numerical application

4.1. Considered pulse-like non-stationary stochastic process and associated EPSD

The usefulness and applicability of the herein proposed stochastic dynamics approach to study the response of bilinear hysteretic SDOF oscillators exposed to PLGMs is numerically exemplified by considering an appropriately defined EPSD $S(\omega,t)$ in Eq. (23) capturing the salient features of a particular recorded accelerogram. The considered accelerogram is the El Centro Array #6 component recorded during the 1979 Imperial Valley earthquake plotted in Fig. 2(a) and classified as a PLGM in [3] as is characterized by a single dominant distinctive pulse. The LF pulse contained in the considered PLGM is plotted in Fig. 2(b) as extracted by Baker [3] (http://web.stanford.edu/~bakerjw/), while Fig. 2(c) plots the residual HF part. Moreover, the pseudo-acceleration response spectrum of the PLGM is plotted in Fig. 2(d) (continuous blue curve) attaining significantly large spectral acceleration values at long natural periods (T>3s) which is a manifestation of the rather rich LF (pulse-like) content.

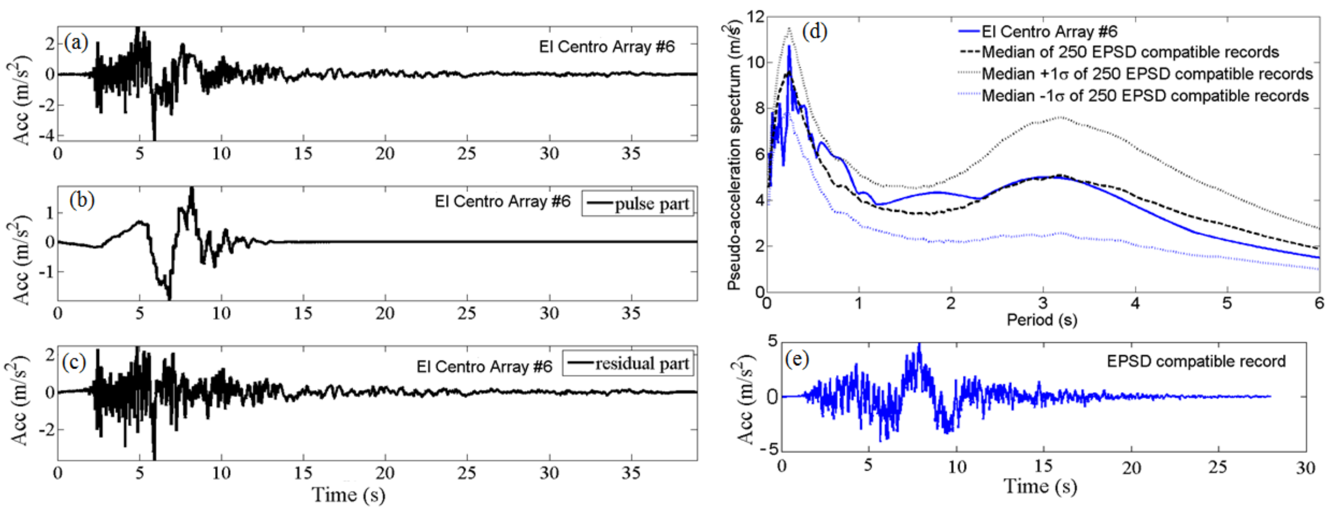

Fig. 2 – (a) to (c): Time history acceleration traces of the El Centro Array #6 component (1979 Imperial Valley event), pulse, and residual; (d): Elastic pseudo-acceleration response spectra of the El Centro Array #6 record and spectra statistics of 250 EPSD compatible accelerograms; (e): An EPSD compatible accelerogram.

The simplest possible form of the PLGM stochastic model in Eq. (18) is adopted comprising one uniformly modulated process to capture the HF content of the considered ground motion in Fig. 2(c) (R=1) and one uniformly modulated process to capture the LF content of the considered ground motion in Fig. 2(b) (P=1). The 11 parameters required in defining the model are determined as detailed in [16] and reported in Table 1. A contour plot of the associated EPSD in Eq. (23) of the PLGM model is provided in Fig.3 in which warmer colors correspond to larger amplitude values. Two bursts of energy are clearly identified on the time-frequency plane one corresponding to the HF and one to the LF parts of the stochastic model. The former (HF) burst is centered at approximately 18rad/s frequency and 2/b= 4s time instant (HF content) having a relatively low amplittude but being quite widely distributed on the plane. The latter (LF) burst is high amplitude, centered at t_0 = 6.96s time instant, and well localized in the frequency domain at 1.65rad/s.

Table 1 – Parameters defining the adopted PLGM stochastic mode

High frequency part (HF): *R*=1		**Low frequency part (LF): *P*=1**	
e_{HF} - Eq. (20)	**G_{HF} - Eq. (19)**	**e_{LF} – Eq. (22)**	**G_{LF} – Eq. (21)**
C_{HF} = 0.0765 m/s^2 b = 0.5 s^{-1}	ζ_f = 0.55 ω_f = 2.33 rad/s ζ_g = 0.65 ω_g = 22 rad	C_{LF} = 1.1667 m/s2 ω_p = 1.65 rad/s γ = 2.89 t_0 = 6.96 s	ω_p = 1.65 rad/s a = 0.50

To asssess the appropriateness of the considered PLGM stochastic model of using it as a proxy of the recorded PLGM in Fig. 2(a) in applying the stochastic dynamics approach detailed in Section 2, the median elastic response spectrum of an ensemble of 250 realizations (i.e., artificial PLGMs; an arbitrarily chosen one is plotted in Fig. 2(e)) compatible with the EPSD of the PLGM model in Eq.(23) are plotted in Fig. 2(d). These records have been generated by taking the steps delineated in Fig. 1. Specifically, the stationary HF spectrum compatible signals were simulated by filtering white noise sequences through an appropriately defined discrete-time auto-regressive-moving-average filter fitted to the CP spectrum of Eq. (19) as detailed in [26], while the stationary LF spectrum compatible signals were simulated using the standard spectral representation algorithm [29]. Each record is base-line adjusted by acausal high-pass filtering with a fourth-order Butterworth filter with cut-off frequency of 0.13Hz to eliminate spurious low frequencies (see also [26]). It is observed that the above median response spectrum lies close to the response spectrum of the recorded PLGM, especially in the range of long periods (T>2s). Note that enhanced matching in the shorter period range can be achieved by adopting a more refined HF part in the PLGM model (i.e., with R>1), (see also [20]). However, this study focuses moslty on long period yielding structures for which PLGMs are usually detrimental, and for this purpose the achieved level of matching between the median response spectrum of EPSD compatible accelerograms and the response spectrum of the considered recorded PLGM is deemed satisfactory. As a final note on Fig. 2(d), the median plus/minus one standard deviation (±1σ) response spectra of the EPSD compatible accelerograms are also plotted to illustrate the variability in terms of peak linear structural response involved in these simulated signals.

4.2. Time-varying equivalent linear properties (ELPs)

The EPSD $S(\omega,t)$ of the PLGM stochastic model/process defined by the parameters of Table 1 is herein used as input to the stochastic dynamics approach presented in Section 2 to derive time-varying ELPs of yielding bilinear hysteretic SDOF oscillators, that is, ω_{eq} and β_{eq} in Eq. (7). To this aim, $S(\omega,t)$ enters Eq. (17) and the latter is numerically solved in conjunction with Eqs. (7) and (11) for bilinear oscillators of different properties to obtain the variance of the response displacement $\sigma_u^2(t)$, and time-varying ELP statistics. Figures 3 and 4 furnish selected plots of these quantities in time to demonstrate that the derived ELPs from the herein proposed approach are amenable to a physically meaningful interpretation and are not simply mathematical/numerical artefacts.

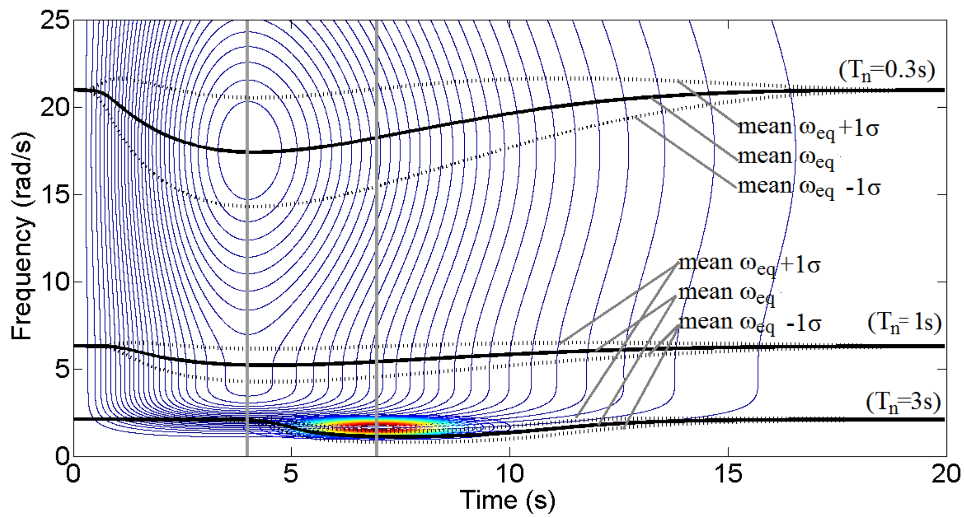

Fig. 3 – Pulse-like input EPSD contour plot and time-varying ω_{eq} statistics for three bilinear hysteretic oscillators with ξ_o=5%, α=0.1, and R=5 and different pre-yield natural periods T_n.

Specifically, in Fig. 4 the mean and the mean ±1σ values of ω_{eq} are plotted on the time-frequency plane for three inelastic oscillators with different pre-yield natural period T_n= 2π/ω_o equal to 0.3s, 1s, and 3s, and with common damping ratio ξ_o=5% and post over pre-yielding stiffness α=0.1. The yielding displacement u_y of all oscillators is set such that they the same strength reduction factor $R=\max_t\left\{\left|f_{el}(t)\right|\right\}/f_y=\max_t\left\{\left|u_{el}(t)\right|\right\}/u_y=5$, where $\max_t\left\{\left|u_{el}(t)\right|\right\}$ is hereafter computed for any given inelastic oscillator by the mean peak response displacement of a linear SDOF oscillator with damping ratio ξ_o and natural frequency ω_o exposed to the ensemble of 250 EPSD compatible artificial pulse-like accelerograms whose response spectra statistics are shown in Fig. 2(d). To facilitate interpretation, the plots of the ω_{eq} ELP are superposed on the contour plot of the input EPSD and the two vertical gray lines indicate the time instants at which the two prominent bursts of energy are centered: the HF burst at 2π/18= 0.35s period and the LF burst at 2π/1.65= 3.8s period. These plots confirm that the equivalent natural frequency ω_{eq} obtained by the adopted approach can be interpreted as an instantaneous stiffness index of the inelastic oscillators since its value decreases due to yielding at times where the oscillators are exposed to the strong ground motion part of the input stochastic process. More importantly, it can be deduced from Fig.4 that the proposed stochastic dynamics approach captures faithfully, through the time-varying ω_{eq} ELP, the impact of the salient non-stationary features of the input PLGM process on the inelastic response of the bilinear oscillators in *both* the time *and in the frequency domain*. Indeed, the stiffer oscillator is significantly excited (and yields) relatively early in time due to the HF burst of energy which peaks at a period, 0.35s, close to the pre-yield natural period of the oscillator. This is manifested by a local reduction of the ω_{eq} in time which traces well the shape of the HF burst and attains a local minimum very close to the local peak value of the EPSD corresponding to the HF part of the input process. However, the flexible oscillator with a T_n (=3s) value lying close to the pulse period of 3.8s yields approximately 3s later in time from the stiff oscillator (as manifested by a reduction to the ω_{eq}) as its response is almost exclusively governed by the LF burst of energy which peaks 3s later than the HF burst. The third considered oscillator with an intermediate pre-yield stiffness is mostly influenced by the HF burst, however, it does yield somewhat later in time than the stiff oscillator: an indication that it is affected to a small degree by the LF content of the input stochastic process.

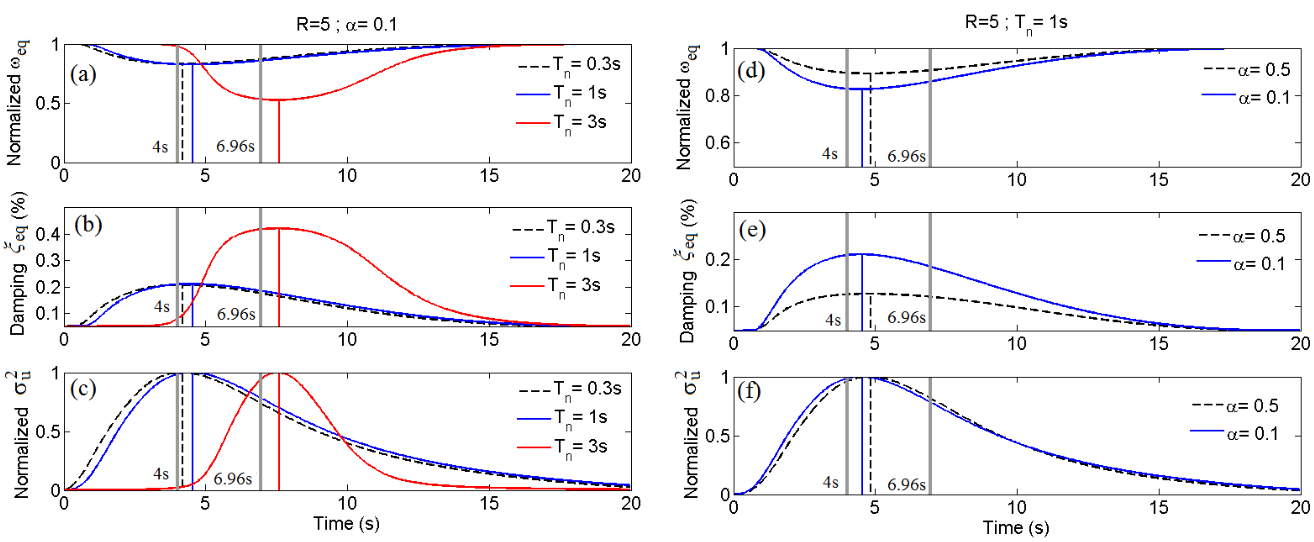

Fig. 4 – Time-varying mean ELPs and response displacement variance $\sigma_u^2(t)$ for various bilinear oscillators with ξ_o=5% exposed to the EPSD in Fig.3.

The above observations are further confirmed by examining Fig.4(a) which plots the mean ω_{eq} in time normalized to its peak (pre-yielding) value of the previously considered inelastic oscillators. The location of the minimum ω_{eq} values, which coincide with the time instant at which the response variance is maximized (Fig. 4(c)), are also indicated with vertical lines. As intuition suggests, the local mean ω_{eq} minima or, equivalently, the local $\sigma_u^2(t)$ maxima, occur with some delay from the two local maxima of the seismic input energy also shown in these plots by vertical gray lines. Moreover, Fig.4(b) plots the corresponding equivalent mean damping ratio defined as $\xi_{eq}= \beta_{eq}/(2\omega_{eq})$. It is seen that ξ_{eq} has a reciprocal relationship with ω_{eq}: when ω_{eq} decreases, ξ_{eq} increases and *vice versa*, while local extreme values are attained at exactly the same time. Effectively, these numerical data suggest that equivalent damping ratio values larger than the initial ξ_o= 5% value are associated with an instantaneous hysteretic energy dissipation and is a manifestation of non-linear behavior. Additional evidence of the fact that ω_{eq} and ξ_{eq} bear intuitive physical significance and are well-related with the severity of the exhibited non-linear response to non-stationary PLGM excitations is provided in the right panel plots of Fig.4 pertaining to two bilinear osicllators with different post-to-pre-yielding stiffness ratio α and all other properties the same. The oscillator with hysteretic behavior closer to a perfectly elasto-plastic one (α=0.1) attain lower equivalent natural frequency and higher equivalent damping ratio values at all time instants compared to the oscillator with α=0.5 for the same strength reduction R=5, while the maxima of the ELPs occur later in time.

4.3. Estimation of peak ductility demand using statistics of ELP maxima

Having established the physical meaning of the ELPs of Eq. (7) in interpreting the severity and the attributes of the non-linear behavior of bilinear hysteretic osicllators exposed to PLGM action, a further step is herein taken to illustrate the usefulness and potential of using the ELSs defined by statistics of the ELP maxima in time, to predict the peak non-linear response for different levels of input excitation (i.e., within an incremental dynamic analysis framework) or, equivalently, for different yielding strength (or displacement) as defined by the strength reduction factor R. To this end, Figs. 5(a) and 5(b) plot the mean and the mean ±1σ of the peak values of the ELPs (occuring at different times for each R value when $\sigma_u^2(t)$ is maximum as shown in Fig. 4) as functions of the strength reduction factor R for a bilinear oscillator with α=0.1 and T_n=1s. As R increases, i.e., as bilinear oscillators with lower yielding strength are considered or, equivalently, as the seismic input intensity increases, ω_{eq} decreases monotonically yielding softer ELSs, while ξ_{eq} increases to account for the increased energy dissipation through more severe plastic/ hysteretic behaviour of the inelastic oscillators. However, the rate of both the above trends tend to saturate for larger R values. Such trends have been observed in the literature in the context of standard statistical linearization techniques assuming stationary input excitation and yielding deterministically defined ELPs [21,22].

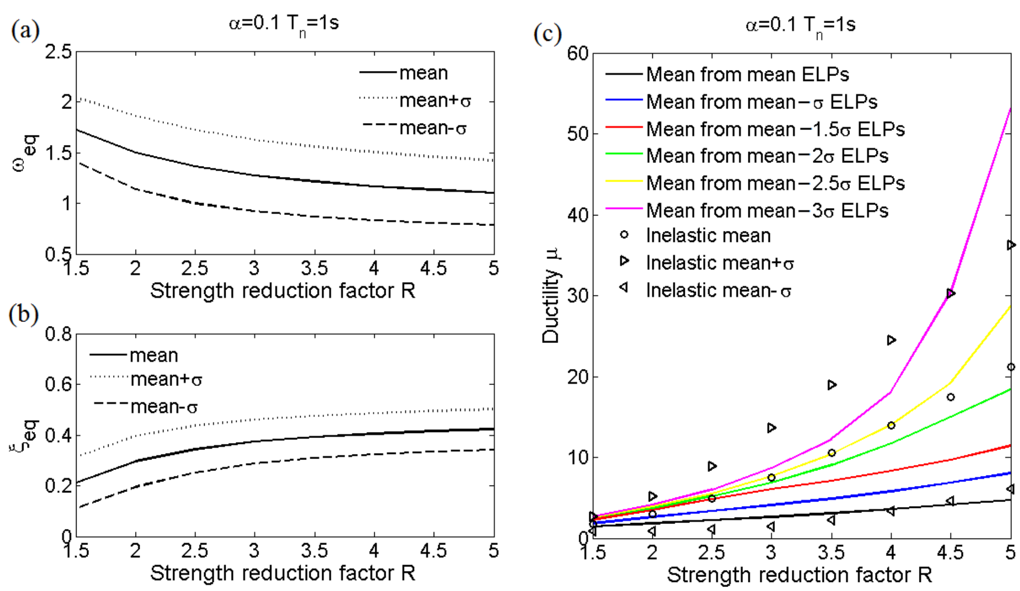

Fig. 5 – ELPs for bilinear oscillator with a= 0.5, ωo= 2π rad/s, and various yielding displacement uy Peak response of various bilinear hysteretic oscillators and of the corresponding equivalent linear oscillators for 40 EC8 compatible accelerograms.

Next, statistical values of the peak absolute ductility $\mu = \max_t \{|u(t)|\} / u_y$, are plotted versus the strength reduction factor R in Fig. 5(c) (dots of various shapes) for bilinear hysteretic oscillators with α=0.1, T_n=1s, and different yielding displacements u_y obtained from standard NRHA. The analysis uses the standard constant acceleration Newmark algorithm and is undertaken for the ensemble of the 250 simulated PLGMs discussed in sub-section 4.1. (Figs. 2(d) and 2(e)). Superposed on Fig. 5(c), is the peak response $y(t)$ normalized by the yielding deformation u_y of equivalent linear oscillators (curves of various types) defined by different peak ELP statistical values. It is seen that the average of the peak nonlinear responses can be well-approximated by the peak response of ELSs defined by the mean ELP values reduced by 2 to 2.5 their standard deviation σ. Similar results and trends not reported here due to space limitations hold for bilinear oscillators with various different properties as well. Overall, these results suggest that the adopted stochastic dynamics technique may provide useful estimates of the peak response statistics of bilinear oscillators exposed to PLGMs without the need for NRHA.

5. Concluding remarks

A non-stationary stochastic averaging/linearization formulation was considered in conjunction with a phenomenological stochastic PLGM model to study the response of hysteretic bilinear oscillators to typical pulse-like near-source accelerograms with forward-directivity low frequency pulses without resorting to non-linear response history analysis. This was achieved by focusing on the time-varying ELPs derived from the proposed methodology treated as non-stationary stochastic processes. The evolutionary statistics of the ELPs (mean value and standard deviation) depend on the properties of the bilinear oscillator and on the features of the excitation stochastic model. The latter captures the time-evolving intensity and frequency content signatures of typical PLGMs by means of a parametrically defined non-separable non-stationary stochastic process given by the sum of separable uniformly modulated stochastic processes interpreted as local bursts of energy with different locations on the time-frequency plane. It was numerically demonstrated by considering a PLGM stochastic process fitted to a typical fault-normal recorded accelerogram with a single forward-directivity signature (low-frequency pulse), that the obtained ELPs are amenable to a clear physical interpretation. They can be construed as instantaneous (time-varying) effective stiffness and viscous damping characterizing the time-varying inelastic response level/behavior whose severity is governed by resonance structural dynamics phenomena related to the input seismic energy distribution on the time-frequency plane and to the pre-yield natural period of the bilinear oscillators. Furthermore, it has been verified in the context of Monte Carlo analysis pertaining to an ensemble of 250 simulated PLGM records compatible with the adopted PLGM stochastic model that the peak inelastic response of bilinear oscillators can be well approximated by the peak response of equivalent linear oscillators defined by appropriate statistics of ELPs evaluated at the time instant when the response variance determined by the adopted approach is maximized. Future extensions of this work will involve the study of the inelastic response of yielding multi-degree-of-freedom hysteretic structural systems exposed to PLGMs through surrogate linear oscillators [30] as well as the extention of the approach for stochastic incremental dynamic analysis [31].

6. References

[1] Somerville PG, Smith NF, Graves RW, Abrahamson NA (1997): Modification of empirical strong ground motion attenuation relations to include the amplitude and duration effects of rupture directivity. *Seismological Research Letters*, **68**, 199–222.

[2] Mavroeidis G, Papageorgiou AS (2003): A mathematical representation of near-fault ground motions. *Bulletin of Seismological Society of America*, **93**, 1099–1131.

[3] Baker JW (2007): Quantitative classification of near-fault ground motions using wavelet analysis. *Bulletin of the Seismological Society of America*, **97** (5), 1486-1501.

[4] Xu Z, Agrawal A (2010): Decomposition and effects of pulse components in near-field ground motions. *Journal of Structural Engineering*, **136** (6), 690-699.

[5] Tang Y, Zhang J (2011): Response spectrum-oriented pulse identification and magnitude scaling of forward directivity pulses in near-fault ground motions. *Soil Dynamics and Earthquake Engineering*, **31** (1), 59-76.

[6] Bertero VV, Mahin SA, Herrera RA (1978): A seismic design implication of near-fault San Fernando earthquake records. *Earthquake Engineering & Structural Dynamics*, **6**, 31–42.

[7] Hall JF, Heaton TH, Halling MW, Wald DJ (1995): Near-source ground motions and its effects on flexible buildings. *Earthquake Spectra*, **11** (4), 569–605.

[8] Sehhati R, Rodriguez-Marek A, El Gawady M, Cofer WF (2011): Effects of near-fault ground motions and equivalent pulses on multi-story structures. *Engineering Structures,* **33** (3), 767-779.

[9] Tothong P, Cornell CA (2008): Structural performance assessment under near-source pulse-like ground motions using advanced ground motion intensity measures. *Earthquake Engineering and Structural Dynamics*, **37** (7), 1013-1037.

[10] Champion C, Liel A (2012): The effect of near-fault directivity on building seismic collapse risk. *Earthquake Engineering and Structural Dynamics*, **41**, 1391–1409.

[11] Baltzopoulos G, Vamvatsikos D, Iervolino I (2016): Analytical modelling of near-source pulse-like seismic demand for multi-linear backbone oscillators. *Earthquake Engineering & Structural Dynamics*, DOI: 10.1002/eqe.2729.

[12] Taflanidis AA, Jia G (2011): A simulation-based framework for risk assessment and probabilistic sensitivity analysis of base-isolated structures. *Earthquake Engineering and Structural Dynamics*, **40** (14), 1629-1651.

[13] Moustafa A, Takewaki I (2010): Deterministic and probabilistic representation of near-field pulse-like ground motion. *Soil Dynamics and Earthquake Engineering*, **30,** 412–422.

[14] Kougioumtzoglou IA, Spanos PD (2009): An approximate approach for nonlinear system response determination under evolutionary stochastic excitation. *Current Science, Indian Academy of Sciences*, **97** (8), 1203-1211.

[15] Tubaldi E, Kougioumtzoglou IA (2015): Nonstationary stochastic response of structural systems equipped with nonlinear viscous dampers under seismic excitation. *Earthquake Engineering & Structural Dynamics*, **44**, 121-138.

[16] Lungu A, Giaralis A (2013): A non-separable stochastic model for pulse-like ground motions. *11th International Conference on Structural Safety and Reliability for Integrating Structural Analysis, Risk and Reliability ICOSSAR*, pp. 1017-1024, New York, US.

[17] Caughey TK (1960): Random excitation of a system with bilinear hysteresis. *Journal of Applied Mechanics*, **27**, 649-652.

[18] Roberts JB, Spanos PD (2003): *Random Vibration and Statistical Linearization*. Dover Publications, NY.

[19] Spanos PD, Vargas Loli LM (1985): A statistical approach to generation of design spectrum compatible earthquake time histories. *Soil Dynamics and Earthquake Engineering* **4**, 2–8.

[20] Conte JP, Peng BF (1997): Fully nonstationary analytical earthquake ground-motion model. *Journal of Engineering Mechanics ASCE*, **123**, 15–24.

[21] Giaralis A, Spanos PD (2010): Effective linear damping and stiffness coefficients of nonlinear systems for design spectrum based analysis. *Soil Dynamics and Earthquake Engineering*, **30**, 798-810.

[22] Spanos PD, Giaralis A (2013): Third-order statistical linearization-based approach to derive equivalent linear properties of bilinear hysteretic systems for seismic response spectrum analysis. *Structural Safety*, **44**, 59-69.

[23] Suzuki Y, Minai R (1988): Application of stochastic differential equations to seismic reliability analysis of hysteretic structures. *Probabilistic Engineering Mechanics*, **3**, 43-52.

[24] Spanos PD (1978): Non-stationary random vibration of a linear structure. *International Journal of Solids and Structures*, **14**, 861-867.

[25] Soong TT (1973): *Random Differential Equations in Science and Engineering*. Academic Press, NY.

[26] Giaralis A, Spanos PD (2009): Wavelets based response spectrum compatible synthesis of accelerograms- Eurocode application (EC8). *Soil Dynamics and Earthquake Engineering*, **29**, 219-235.

[27] Spanos PD, Giaralis A, Jie L (2009): Synthesis of accelerograms compatible with the Cjinese GB 50011- 2001 design spectrum via harmonic wavelets: artificial and historic records. *Earthquake Engineering and Engineering Vibrations*, **8**, 189–206.

[28] Spanos PD, Zeldin BA (1998): Monte Carlo treatment of random fields: a broad perspective. *Applied Mechanics Reviews* **51**, 219–37.

[29] Shinozuka M, Deodatis G (1991): Simulation of stochastic processes by spectral representation. *Applied Mechanics Reviews*, **44** (4), 191-204.

[30] Kougioumtzoglou IA, Spanos PD (2013): Nonlinear MDOF system stochastic response determination via a dimension reduction approach. *Computers and Structures*, **126**, 135-148.

[31] Dos Santos KRM, Kougioumtzoglou IA, Beck AT (2016): Incremental Dynamic Analysis: A Nonlinear Stochastic Dynamics Perspective. *Journal of Engineering Mechanics*, DOI: 10.1061/(ASCE)EM.1943-7889.0001129.